Capillarity

Vol. 13, No. 2, p. 29-36, 2024

Original article

Pore-scale mechanism of coupled pressure-driven flow and spontaneous imbibition in porous media during high-pressure water injection processes

Debin Kong[1]*, Yingfeng Peng[2,3], Zhenyu Zhou[1], Huanhuan Peng[2], Zhewei Chen[2,3]

[1]School of Civil and Resources Engineering, University of Science and Technology Beijing, Beijing 100083, P. R. China

[2]PetroChina Research Institute of Petroleum Exploration & Development, Beijing 100083, P. R. China

[3]State Key Laboratory of Continental Shale Oil, Daqing 163412, P. R. China

Keywords:
High-pressure injection
pressure-driven flow
spontaneous imbibition
residual oil

Cited as:
Kong, D., Peng, Y., Zhou, Z., Peng, H., Chen, Z. Pore-scale mechanism of coupled pressure-driven flow and spontaneous imbibition in porous media during high-pressure water injection processes. Capillarity, 2024, 13(2): 29-36.
https://doi.org/10.46690/capi.2024.11.01

Abstract:
During the development of low-permeability oil fields, high-pressure water injection is employed as a means of increasing reservoir pressure and enhancing oil recovery. This process features an interplay between pressure-driven flow and spontaneous imbibition, which exerts a pivotal influence on the distribution of oil and water. To describe the dynamics of this interplay, pore-scale visualization experiments and core flooding online nuclear magnetic resonance experiments were conducted in the present work. The results demonstrate that after water flooding, residual oil predominantly exists in clustered forms. Initially, during high-pressure water injection and the early stages of well shut-in, crude oil movement is driven primarily by pressure. As the process continues, however, a spontaneous imbibition mechanism driven by capillary forces becomes the predominant force, which results in the transformation of clustered residual oil into various mobilizable forms. This reorganization of residual oil is a migration pattern from smaller to larger pores, facilitated by spontaneous imbibition.

1. Introduction

When a low-permeability reservoir enters the mature stage of field development, the formation pressure gradually decreases, resulting in a continuous decline in well production capacity, limiting the economic and effective development of the reservoir (Dikken, 1990). The method of high-pressure water injection supplements formation pressure in a low-permeability reservoir. The effect of supplementing formation pressure is achieved by rapidly injecting water with large fluid volume and then shutting down the well, along with the surrounding wells. Thus, the flow capacity and imbibition effect of crude oil are improved, oil and water are redistributed in the reservoir, the development efficiency of the reservoir is enhanced, and increased production can be realized (Carpenter, 2013; Da et al., 2021; Lei et al., 2024).

During the process of high-pressure water injection, the main mechanisms of flow are coupled pressure-driven flow (viscous flow) and spontaneous imbibition. Unveiling the unclear mechanisms of this coupled flow is a major concern for both scholars and field engineers. To supplement the depleted reservoir pressure, the energy storage fracturing technology of energization, fracturing, shut-in, and flowback is adopted. The combination of energy supplement before fracturing and fracturing transformation, along with the combination of imbibi-

Yandy Scientific Press

*Corresponding author.
E-mail address: kongdb@ustb.edu.cn (D. Kong); pengyf21@petrochina.com.cn (Y. Peng); zzy18769938315@163.com (Z. Zhou); phh21@petrochina.com.cn (H. Peng); chenzw20@petrochina.com.cn (Z. Chen).

Received July 11, 2024; revised August 9, 2024; accepted September 4, 2024; available online September 10, 2024.

tion displacement and well plugging after fracturing can solve the problems of low formation pressure, significant energy loss, low production rate, and low energy production ratio in the traditional hydraulic fracturing process of low-permeability reservoirs (Zou et al., 2021; Li et al., 2022). Reservoir pressure is an important factor affecting the imbibition effect. During the shut-in process after high-pressure water injection, the injected water induces the fracture to open and enters the matrix from the fracture to form a two-phase-flow area. With the expansion of the area affected by the pressure difference, according to the different dominant forces, the two-phase flow area is divided into a two-phase flow area dominated by pressure difference and accompanied by imbibition (capillary force) and a two-phase flow area dominated by imbibition (Karimaie et al., 2006; Jiang et al., 2021).

Spontaneous imbibition plays a key role after high-pressure water injection. Therefore, studying the migration law and mechanism of imbibition displacement can help to derive methods for improving oil recovery (Mattax and Kyte, 1962; Morrow and Mason, 2001; Cai et al., 2023). The most classical and widely used model to describe imbibition displacement is the Lucas-Washburn equation (Lucas, 1918; Washburn, 1921). Based on the capillary flow model, Rangel-German and Kovscek (2006) used the microscopic model to study the flow law of water in matrix-fractured media. Cai et al. (2021) summarized recent years' research progress on the modification and extension of Lucas-Washburn equation in various microchannels and porous media. Many scholars have studied the effects of physical properties (porosity, permeability, pore structure), fluid properties (viscosity, salinity), wettability, and gravity on imbibition by experiments, numerical simulation and analytical methods (Strand et al., 2008; Guo et al., 2020; Wang et al., 2023a; Zhou et al., 2022, 2024).

At present, the research on the law of imbibition replacement of tight cores mainly focuses on spontaneous imbibition and forced imbibition. An analytical solution of spontaneous imbibition and forced imbibition while considering viscous coupling was proposed by Andersen et al. (2020). Tu and Sheng (2020) studied the effects of different soaking pressures on permeability and wettability by numerical simulation. Wang et al. (2023b) proposed a self-similar analytical solution of spontaneous and forced flow in porous media by introducing a conversion variable and a capillary fractional stream function, which they used to simulate the split function of the Buckley-Leverett solution of viscous flow in porous media. Liu et al. (2022) carried out numerical simulations of forced imbibition in three natural rocks at four different injection rates based on the color-gradient lattice Boltzmann model. In their work, the interfacial evolution and in-situ fluid distribution were analyzed from several perspectives. Jia et al. (2024) used the Shan-Chen lattice Boltzmann model to simulate fluid exchange at the pore scale during the fracturing-shut-in-flowback process. At present, nuclear magnetic resonance (NMR) technology is mostly used in forced imbibition experiments of tight cores under pressure to convert T_2 relaxation time into pore size, so as to study the influence of various influencing factors (pressure, injection rate, interfacial tension, soaking time, permeability, pore size, etc.) on oil recovery (Mai and Kantzas, 2007; Dai et al., 2019; Dou et al., 2021; Cao et al., 2022).

Despite the above progress, there are still shortcomings in studying the law of forced imbibition of tight cores under pressure. The amount of imbibition displacement at the core scale is less, and physical simulation experiments are carried out under pressurized conditions. Furthermore, accurate measurement is difficult to achieve when using the conventional volume method and the mass method. The tight core has obvious stress sensitivity characteristics under the condition of overburden pressure, and whether the change of pore structure will affect the imbibition replacement effect is unknown. The imbibition replacement process cannot be directly observed under pressurized conditions. Using the visual microfluidic model, the migration process and capture mechanism of micro-scale pressure imbibition can be observed more intuitively, and the coupling mechanism of pressure-driven flow and self-priming can be analyzed (Hatiboglu and Babadagli, 2008; Karadimitriou and Hassanizadeh, 2012; Jafari et al., 2017).

Based on a pore-scale visualization experiment and core flooding online NMR experiment, this study comprehensively analyzed the flow mechanism after high-pressure water injection and energy storage according to the process of 'energy-increasing, fracturing, shut-in, and backflow' energy storage fracturing. The oil-water two-phase flow law in porous media was analyzed by core-scale online NMR, which was compared with a pore-scale visualization experiment. It is of practical significance to study the coupling law of pressure drive and self-priming in the process of high-pressure water injection, evaluate the effect of oil recovery improvement, and improve the economic benefits.

2. Experimental method and procedures

2.1 Materials

The experimental crude oil was a mixture of dead oil and kerosene in a certain ratio in the P oil field, with a viscosity of 5 mPa·s at 25 °C. Experimental brine was prepared according to the salinity composition specified in Table 1.

Experimental cores were selected from ultra-low permeability sandstone cores produced from P oil fields, whose physical properties are listed in Table 2.

Pore-scale visualization experiments were carried out using a microfluidic chip made of polydimethylsiloxane, and the geometry within the microfluidic chip was formed based on scanning electron microscope images of ultra-low-permeability sandstones, as depicted in Fig. 1. The pore throat radii in microfluidic chips mainly ranged from 1 to 61 μm and depths of 10 μm.

2.2 Procedures

2.2.1 Pore-scale visualization experiment

The specific pore-scale visualization experimental steps shown in Fig. 2 were as follows:

1) Inject the crude oil into the microfluidic chip until it fills the pores.
2) Perform the water flooding by experimental brine at a

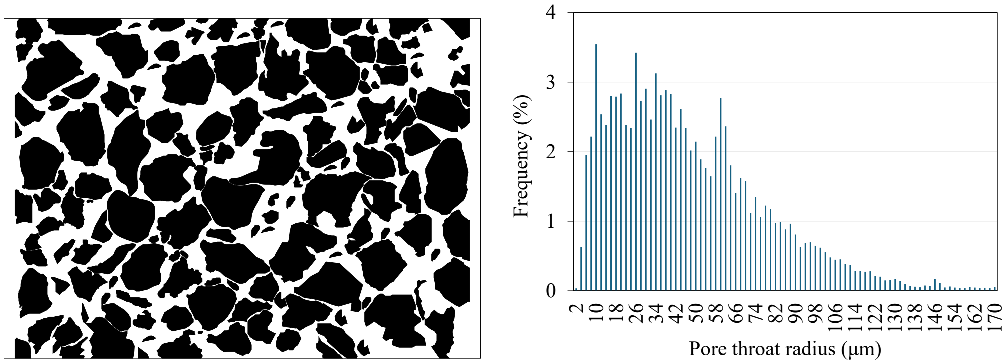

(a) (b)

Fig. 1. (a) Schematic diagram and (b) pore throat radius of microfluidic chip.

Table 1. Salinity composition of simulation brine.

$K^+ + Na^+$ (mg/L)	Ca^{2+} (mg/L)	Mg^{2+} (mg/L)	$HCO_3{}^-$ (mg/L)	Cl^- (mg/L)	$SO_4{}^{2-}$ (mg/L)	$CO_3{}^{2-}$ (mg/L)	Total salinity (mg/L)
2,294.23	33.67	16.34	2,914.49	1,883.14	37.66	-	7,179.52

Table 2. Core physical properties.

No.	Length (cm)	Diameter (cm)	Rock density (g/cm^3)	Porosity (%)	Permeability (mD)
P333	7.6635	2.525	2.242	15.948	0.3012

constant rate of 5 μL/min until no oil flows out of the outlet, in order to obtain the distribution of residual oil after water flooding.

3) Close the outlet end and continue to inject simulated water at a rate of 1 μL/min for 5 ~ 10 minutes to build up higher pressure for energy storage. Then, stop the water injection and close the inlet and outlet for 2 hours.
4) After 2 hours of standing time, continue to close the inlet and open the outlet for backflow for 20 minutes.

2.2.2 Core flooding online NMR experiment

During the core flooding experiments, the high-capacity MRI system (LIME-MRI-D12, Beijing Limecho Technology Co., Ltd) was used to measure the NMR T_2 spectrum, and a CPMG sequence was selected. To differentiate the NMR signal of water from that of oil, a synthetic brine was prepared with deuterium oxide. The density of the mineralized deuterium oxide was 1.107 g/cm^3 and its viscosity was 1.25 mPa·s at 25 °C. The experimental setup process is shown in Fig. 3, with the specific experimental steps briefly described as follows:

1) Evacuate the cores for 12 hours and subsequently inject them with crude oil at a rate of 0.05 mL/min for 12 hours. Determine the saturated oil mass and porosity of the core by weighing, then measure the NMR T_2 spectrum of the core after saturating the crude oil.
2) Place the core back into the core holder and set the confining pressure to 17 MPa. The displacement starts at a constant pressure of 13.5 MPa with mineralized deuterium oxide until the water cut of the produced fluids exceeds 98% or the oil volume of the produced fluids no longer increases. Measure the NMR T_2 spectrum of the core at the end of water flooding.
3) Increase the injection pressure to 15 MPa with mineralized deuterium oxide for storage, then set the outlet back pressure to 15 MPa. Shut in the outlet for 12 hours, and measure the NMR T_2 spectrum of the core at 2, 4, 6, 8 and 12 hours after the start of shut-in.
4) After 12 hours, reduce the back pressure to 10 MPa to fluid out, and after 1 hour, reduce the back pressure again to 0 MPa to fluid out. Measure the NMR T_2 spectrum of the core after each pressure reduction.

3. Results and discussion

3.1 Pore-scale visualization experiment

3.1.1 Characteristics of residual oil distribution

As illustrated in the real-time images of the pore-scale visualization experiment presented in Fig. 4, after the water flooding stage, the injected water forms a dominant channel, creating the bypass oil. During the shut-in stage, the distribution of residual oil in the microfluidic chip is reconstructed at a gradual pace due to the coupling of pressure-driven flow and spontaneous imbibition. In the initial period, pressure-driven flow is the predominant mechanism, which is accompanied by

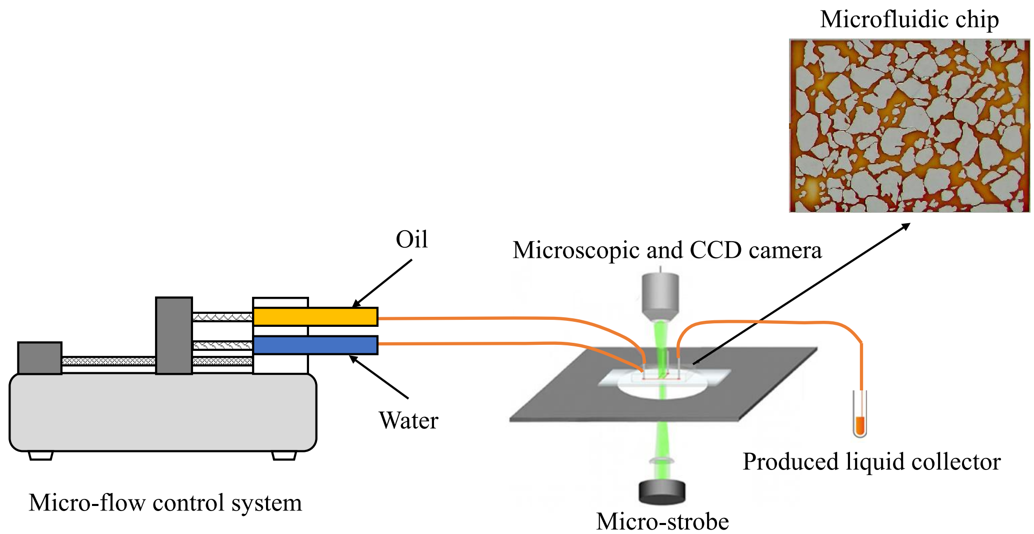

Fig. 2. Diagram of the pore-scale visualization experimental setup.

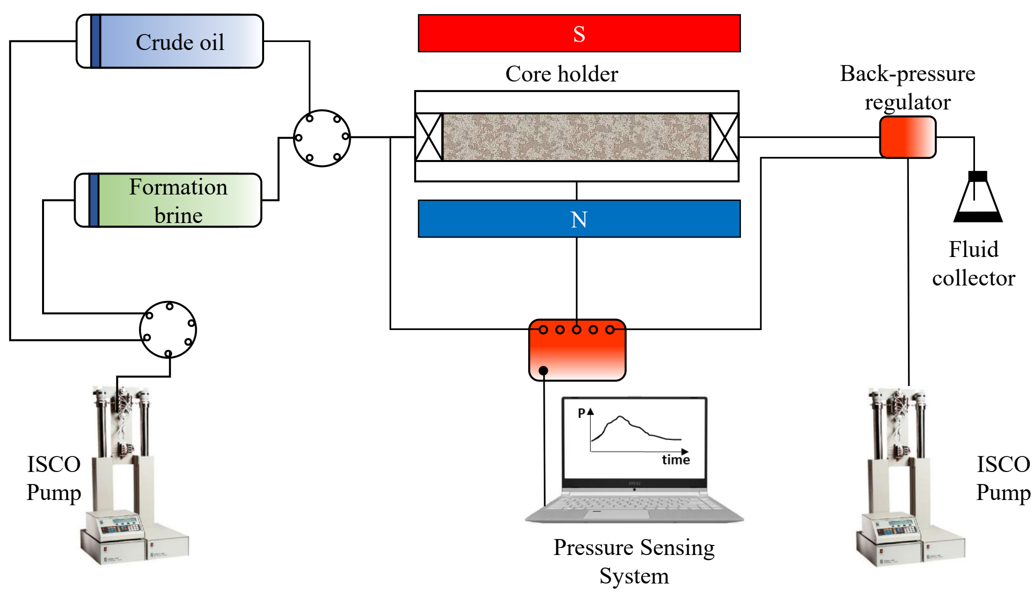

Fig. 3. Diagram of experimental setup of core flooding online NMR.

spontaneous imbibition. Once the pressure difference within the microfluidic chip has reached a stable state, the pressure-driven flow ceases, and spontaneous imbibition becomes the dominant process in the reconstruction of residual oil. This results in the displacement of the crude oil from small pores to large pores, leading to a change in the distribution of the remaining oil. After the outlet is opened again, the crude oil is extracted due to the combined effect of pressure and capillary force.

The recovery degree can be calculated based on the area percentage occupied by the crude oil in the image. Due to increased pressure, the polydimethylsiloxane material is slightly deformed during well shut-in. Therefore, the deformation of the microfluidic chip is not considered in the determination of residual oil saturation, which is recognized only based on the image. The calculation shows that the recovery degree after water flooding and after energy storage shut-in is 40.55% and 58.99%, respectively, so the high-pressure water injection and energy storage shut-in can improve the oil recovery degree by 18.44%.

Residual oils were classified according to the method of Gao et al. (2020). As shown in Fig. 5, the residual oil types after water flooding are mainly clustered, columned, blind (angular), and films. Following the water flooding stage, the residual oil saturation is found to be 38.27% cluster, 7.80% columnar, 6.44% blind, and 6.03% films. After the application of pressure-driven flow, spontaneous imbibition and flowback, the residual oil was reconstructed. The saturation of cluster residual oil shows a decrease to 36.73%, while that of columnar residual oil an increase to 8.60%. Conversely, the saturation of blind residual oil exhibits a decrease to 5.92%, and that of films residual oil an increase to 7.02%.

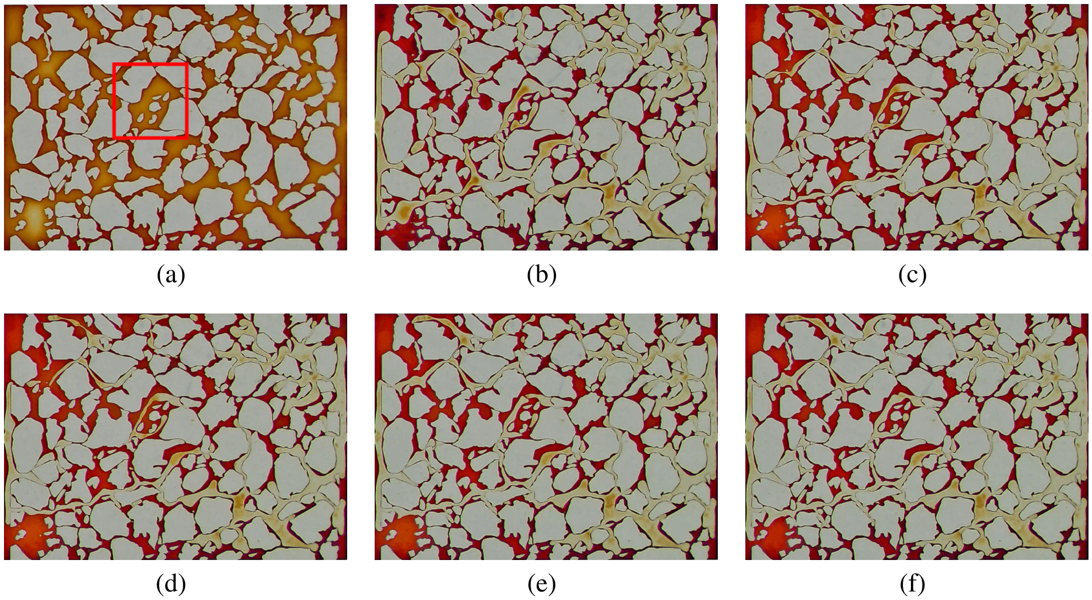

Fig. 4. Real-time images of the pore-scale visualization experiment (a) saturated oil, (b) end of water flooding, (c) 40 min of shut-in, (d) 80 min of shut-in, (e) 120 min of shut-in and (f) end of backflow.

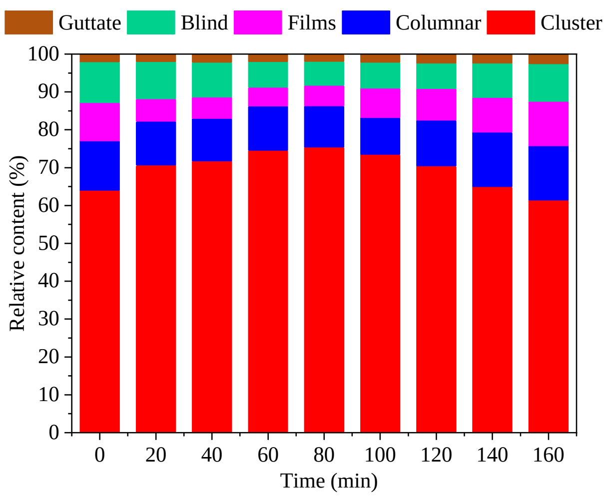

Fig. 5. Changes in the relative content of microscopic residual oil.

3.1.2 Mechanism of microscopic residual oil mobilization

From the changes in the distribution of local residual oil in Fig. 6, the microscopic characteristics of the shut-in process can be observed. From 0 to 20 min shut-in, considered as the initial stage of energy storage, the local residual oil is mainly cluster residual oil (Fig. 6(b)), during which the pressure at the injection end rises rapidly and the local pressure gradient in the pore increases. The residual oil force analysis diagram is shown in Fig. 7, with water droplets entering the pores. The water is exposed to the fluid resistance generated by the pressure difference and the Jamin effect (Tian et al., 2015).

The flow resistance due to the Jamin effect is p_c, p_{c1}, p_{c2} .where p_c represents the Jamin effect flow resistance, p_{c1} represents the pressure at the front of the water droplet, and p_{c2} is the pressure at the end of the water droplet.

In this process, differential pressure produces a driving force greater than the flow resistance. Therefore, the combined force acting on the droplets, i.e., the internal differential pressure, is the main force driving the redistribution of residual oil (Kong et al., 2021).

The period from 40 min to the end of shut-in is the late stage of energy storage. At this stage, spontaneous imbibition plays a dominant role and the microscopic residual oil flows in an intermittent film flow from small pores to large pores. The local cluster residual oil is converted to other types of residual oil (Fig. 6(c)). As shown in Fig. 5, the change in the relative content of microscopic residual oil indicates a decrease in the proportion of cluster residual oil and an increase in the proportion of other types of residual oil. The decrease in the proportion of cluster residual oil, which is difficult to recover during water flooding, facilitates the mobilization of more residual oil during subsequent backflow, thereby increasing the recovery rate.

3.2 Core flooding online NMR experiment

The pores with T_2 relaxation time less than 1 ms are defined as micropores, 1 to 10 ms as ostioles, 10 to 100 ms as mesopores, and more than 100 ms as macropores (Loucks et al., 2012; Zhao et al., 2024). As shown in Fig. 8, a considerable quantity of oil is displaced following water flooding, resulting in a notable reduction in oil volume and an overall rightward shift in the T_2 spectrum. The residual oil in macropores, mesopores, ostioles, and micropores all demonstrate a reduction, with a more pronounced decline observed in micropores. The percentage of crude oil recovered can be calculated from the area difference of the T_2 spectrum, with a water flooding recovery factor of 22.3%.

As shown in Fig. 9, the T_2 spectrum exhibits a gradual

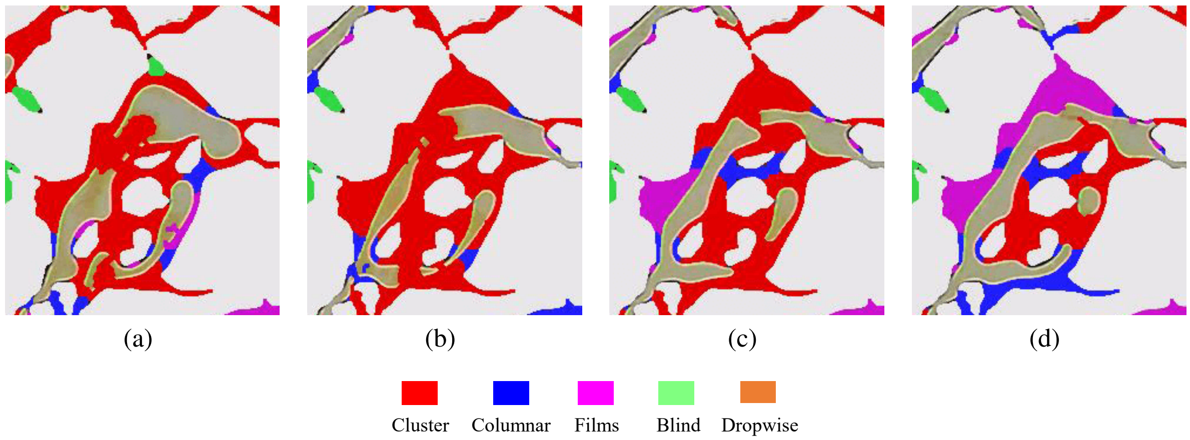

Fig. 6. Transformation of local residual oil (a) end of water flooding, (b) 20 min of shut-in, (c) 120 min of shut-in and (d) end of backflow.

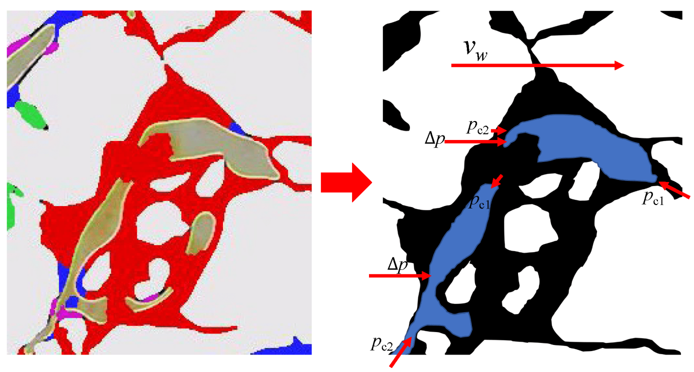

Fig. 7. Force analysis during the early stage of energy storage.

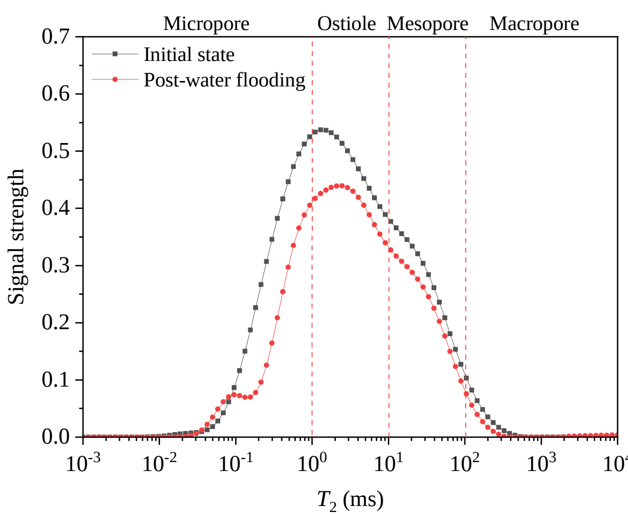

Fig. 8. T_2 spectrum in the water flooding stage.

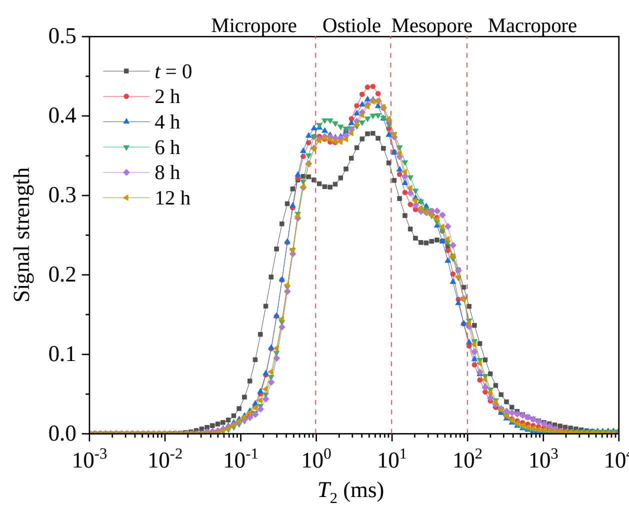

Fig. 9. T_2 spectrum in the energy storage stage.

shift to the right over time. The proportion of residual oil in micropores and macropores is observed to decrease, while that in ostioles and mesopores increases. This indicates that a redistribution of residual oil occurred at this stage. The recovery factor following energy storage and flowback is 39.00%, representing an increase of 16.69% compared to the initial recovery factor.

The coupled effect of pressure-driven flow and spontaneous imbibition forces the residual oil to undergo a redistribution and mobilization process. Fig. 10 illustrates the relative distribution of residual oil in pores of varying sizes. There is a notable decrease in the percentage of oil present in micropores, from 25.78% to 18.43%. Conversely, the percentage in ostioles are increased from 38.7% to 44.63%. The percentage of oil

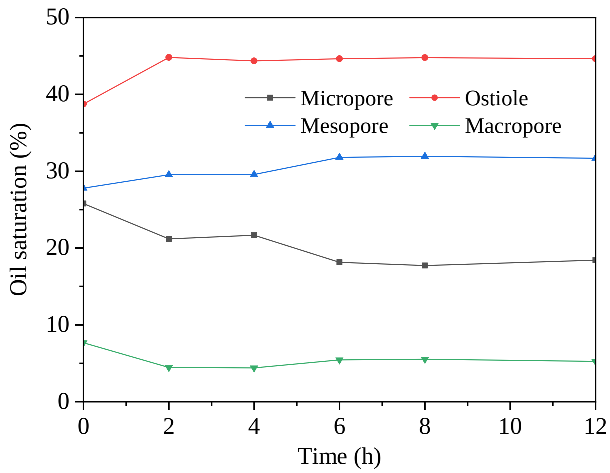

Fig. 10. Saturation curves of various scale pores in the energy storage stage.

in micropores is decreased from 5% to 44.63%, while that in ostioles is increased from 27.81% to 31.68%. Conversely, the oil percentage in macropores is decreased from 7.66% to 5.26%.

4. Conclusions

1) In high-pressure water injection processes, the coupled effect of pressure-driven flow and spontaneous imbibition significantly affects the oil-water distribution.
2) During the initial phase of energy storage, the displacement pressure serves as the primary driving force for crude oil flow, which is predominantly driven by pressure-driven flow mechanisms. In the subsequent stages, capillary force assumes the role of the primary driving mechanism for crude oil, and the dominant process becomes spontaneous imbibition. Clustered residual oil is transformed into columnar, film and blind residual oil states that can be mobilized by water.
3) Residual oil gradually migrates from micropores to ostioles, then to mesopores and finally to macropores by the process of spontaneous imbibition.
4) Following the implementation of reverse flow by high-pressure water injection and energy storage technology, the recovery factor can be increased by 16.69% to 18.44%.

Acknowledgements

The authors acknowledge the financial support of the Natural Sciences Foundation of China (No. 42102163). The authors extend their heartfelt thanks to Dr. Wenbin Gao from the Institute of Rock and Soil Mechanics, Chinese Academy of Sciences, for his invaluable guidance and assistance in the analysis of the data.

Conflict of interest

The authors declare no competing interest.

References

Andersen, P. Ø., Nesvik, E. K., Standnes, D. C. Analytical solutions for forced and spontaneous imbibition accounting for viscous coupling. Journal of Petroleum Science and Engineering, 2020, 186: 106717.

Cai, J., Jin, T., Kou, J., et al. Lucas-Washburn equation-based modeling of capillary-driven flow in porous systems. Langmuir, 2021, 37(5): 1623-1636.

Cai, J., Sun, S., Wang, H. Current advances in capillarity: Theories and applications. Capillarity, 2023, 7(2): 25-31.

Cao, B., Lu, X., Xie, K., et al. The pore-scale mechanisms of surfactant-assisted spontaneous and forced imbibition in water-wet tight oil reservoirs. Journal of Petroleum Science and Engineering, 2022, 213: 110371.

Carpenter, C. Impact of liquid loading in hydraulic fractures on well productivity. Journal of Petroleum Technology, 2013, 65(11): 162-165.

Dai, C., Cheng, R., Sun, X., et al. Oil migration in nanometer to micrometer sized pores of tight oil sandstone during dynamic surfactant imbibition with online NMR. Fuel, 2019, 245: 544-553.

Da, Y., Xue, X., Liu, M. Energy enhancement mechanism of energy storage refracturing in ultra-low permeability oil fields. Science Technology and Engineering, 2021, 21(33): 14139-14146.

Dikken, B. J. Pressure drop in horizontal wells and its effect on production performance. Journal of Petroleum Technology, 1990, 42(11): 1426-1433.

Dou, L., Xiao, Y., Gao, H., et al. The study of enhanced displacement efficiency in tight sandstone from the combination of spontaneous and dynamic imbibition. Journal of Petroleum Science and Engineering, 2021, 199: 108327.

Gao, W., Li, Y., He, S., et al. Classification method of occurrence mode of remaining oil based on fluorescence thin sections. Acta Petrolei Sinica, 2020, 41(11): 1406-1415.

Guo, J., Li, M., Chen, C., et al. Experimental investigation of spontaneous imbibition in tight sandstone reservoirs. Journal of Petroleum Science and Engineering, 2020, 193: 107395.

Hatiboglu, C. U., Babadagli, T. Pore-scale studies of spontaneous imbibition into oil-saturated porous media. Physical Review E, 2008, 77(6): 066311.

Jafari, I., Masihi, M., Nasiri Zarandi, M. Experimental study on imbibition displacement mechanisms of two-phase fluid using micromodel: Fracture network, distribution of pore size, and matrix construction. Physics of Fluids, 2017, 29(12): 122004.

Jiang, Y., Xu, G., Shi, Y. Forced imbibition in tight sandstone cores. Petroleum Geology and Experiment, 2021, 43(1): 144-153. (in Chinese)

Jia, N., Lv, W., Liu, Q., et al. Pore-scale modeling of pressure-driven flow and spontaneous imbibition in fracturing-shut-in-flowback process of tight oil reservoirs. International Journal of Energy Research, 2024, 2024: 3505763.

Karadimitriou, N. K., Hassanizadeh, S. M. A review of micromodels and their use in two-phase flow studies. Vadose Zone Journal, 2012, 11(3): vzj2011.0072.

Karimaie, H., Torsæter, O., Esfahani, M. R., et al. Experimental investigation of oil recovery during water imbibition. Journal of Petroleum Science and Engineering, 2006, 52(1-4): 297-304.

Kong, D., Gao, Y., Sarma, H., et al. Experimental investigation of immiscible water-alternating-gas injection in ultra-high water-cut stage reservoir. Advances in Geo-Energy Research, 2021, 5(2): 139-152.

Lei, Z., Wang, Z., Mu, L., et al. Multi-field reconstruction and multi-driven technology for tight oil EOR. Petroleum Exploration and Development, 2024, 51(1): 152-163.

Li, G., Su, Y., Wang, W., et al. Mathematical model and application of spontaneous and forced imbibition in shale porous media-considered forced pressure and osmosis. Energy & Fuels, 2022, 36(11): 5723-5736.

Liu, Y., Berg, S., Ju, Y., et al. Systematic investigation of corner flow impact in forced imbibition. Water Resources Research, 2022, 58(10): e2022WR032402.

Loucks, R. G., Reed, R. M., Ruppel, S. C., et al. Spectrum of pore types and networks in mudrocks and a descriptive classification for matrix-related mudrock pores. AAPG Bulletin, 2012, 96(6): 1071-1098.

Lucas, R. Rate of capillary ascension of liquids. Kolloid Z, 1918, 23: 15-22. (in German)

Mai, A., Kantzas, A. Porosity distributions in carbonate reservoirs using low-field NMR. Journal of Canadian Petroleum Technology, 2007, 46(7): 30-36.

Mattax, C. C., Kyte, J. R. Imbibition oil recovery from fractured, water-drive reservoir. Society of Petroleum Engineers Journal, 1962, 2(2): 177-184.

Morrow, N. R., Mason, G. Recovery of oil by spontaneous imbibition. Current Opinion in Colloid and Interface Science, 2001, 6(4): 321-337.

Rangel-German, E., Kovscek, A. A micromodel investigation of two-phase matrix-fracture transfer mechanisms. Water Resources Research, 2006, 42(3): W03401.

Strand, S., Puntervold, T., Austad, T. Effect of temperature on enhanced oil recovery from mixed-wet chalk cores by spontaneous imbibition and forced displacement using seawater. Energy & Fuels, 2008, 22(5): 3222-3225.

Tian, Y., Ouyang, C., Cai, X. Study on Jamin effect in the low permeability reservoir. Paper Presented at International Conference on Industrial Technology and Management Science, Tianjin, China, 27-28 March, 2015.

Tu, J., Sheng, J. J. Further investigation of forced imbibition in unconventional oil reservoirs for enhanced oil recovery. Energy & Fuels, 2020, 34(9): 10676-10687.

Wang, H., Cai, J., Su, Y., et al. Imbibition behaviors in shale nanoporous media from pore-scale perspectives. Capillarity, 2023a, 9(2): 32-44.

Wang, X., Wang, S., Wu, W., et al. Coupled pressure-driven flow and spontaneous imbibition in shale oil reservoirs. Physics of Fluids, 2023b, 35(4): 042104.

Washburn, E. W. The dynamics of capillary flow. Physical Review, 1921, 17(3): 273-283.

Zhao, J., Ouyang, W., Hui, B., et al. Experimental study on post-fracture oil-water displacement mechanism of tight sandstone reservoir with nuclear magnetic resonance. Thermal Science, 2024, 28(2A): 1013-1019.

Zhou, Y., Guan, W., Zhao, C., et al. Numerical methods to simulate spontaneous imbibition in microscopic pore structures: A review. Capillarity, 2024, 11(1): 1-21.

Zhou, Y., You, L., Kang, Y., et al. Experimental study of the fracture initiation through the synergy of spontaneous imbibition and hydration of residual fracturing fluids in shale gas reservoirs. Journal of Natural Gas Science and Engineering, 2022, 102: 104577.

Zou, C., Zhao, Q., Wang, H., et al. Theory and technology of unconventional oil and gas exploration and development helps China increase oil and gas reserves and production. Oil Forum, 2021, 40(3): 72-79.